BIOMOLECULES & THERAPEUTICS

Original Article
Biomol Ther 27(5), 457-465 (2019)

Enrichment of Short-Chain Ceramides and Free Fatty Acids in the Skin Epidermis, Liver, and Kidneys of db/db Mice, a Type 2 Diabetes Mellitus Model

Minjeong Kim[1], Haengdueng Jeong[2], Buhyun Lee[2], Yejin Cho[2], Won Kee Yoon[3], Ahreum Cho[1], Guideock Kwon[1], Ki Taek Nam[2,*], Hunjoo Ha[1,*] and Kyung-Min Lim[1,*]

[1]Graduate School of Pharmaceutical Sciences, College of Pharmacy, Ewha Womans University, Seoul 03760,
[2]Severance Biomedical Science Institute, Brain Korea 21 PLUS Project for Medical Science, Yonsei University College of Medicine, Seoul 03722,
[3]Laboratory Animal Resource Center, Korea Research Institute of Bioscience and Biotechnology (KRIBB), Cheongju 28116, Republic of Korea

Abstract

Patients with diabetes mellitus (DM) often suffer from diverse skin disorders, which might be attributable to skin barrier dysfunction. To explore the role of lipid alterations in the epidermis in DM skin disorders, we quantitated 49 lipids (34 ceramides, 14 free fatty acids (FFAs), and cholesterol) in the skin epidermis, liver, and kidneys of db/db mice, a Type 2 DM model, using UPLC-MS/MS. The expression of genes involved in lipid synthesis was also evaluated. With the full establishment of hyperglycemia at the age of 20 weeks, remarkable lipid enrichment was noted in the skin of the db/db mice, especially at the epidermis and subcutaneous fat bed. Prominent increases in the ceramides and FFAs (>3 fold) with short or medium chains (<C26) occurred in the skin epidermis (16NS, 18NS, 24NS, 16NDS, 18NDS, 20NDS, 22NDS, 24NDS, C16:1FA, C18:2FA, and C18:1FA) and the liver (16NS, 18NS, 20NS, 24:1NS, 18NDS, 20NDS, 22NDS, C16:1FA, C18:2FA, C18:1FA), whereas those with very long chains were not affected. In the kidney, only slight increases (<3 fold) were observed for 16NS, 18NS, 20NS, 26NDS, C26FA, and C22:1FA. Consistently, LXRα/β and PPARγ, nuclear receptors promoting lipid synthesis, lipid synthesis enzymes such as elongases 1, 4, and 6, and fatty acid synthase and stearoyl-CoA desaturase were highly expressed in the skin and livers of the db/db mice. Collectively, our study demonstrates an extensive alteration in the skin and systemic lipid profiles of db/db mice, which could contribute to the development of skin disorders in DM.

Key Words: Lipids, Ceramide, Free fatty acid, Diabetes mellitus, Skin barrier function

INTRODUCTION

Hundreds of lipid species occur in the skin epidermis, where they constitute structural components, maintain cutaneous physiology, and participate in the progression of diseases (Kendall *et al*., 2015). In particular, ceramides and free fatty acids (FFAs) are known to be pivotal to the skin barrier function (Joo *et al*., 2010; Park *et al*., 2012; Breiden and Sandhoff, 2014), immune regulation, and inflammation (Kendall and Nicolaou, 2013; Uchida, 2014). FFAs display carbon chains of widely varying lengths (Joo *et al*., 2015), and a huge diversity of ceramides, as many as 342 species in 11 families created by the variety of constituting sphingoid bases and linked FFAs, are known to exist in the skin epidermis (Masukawa *et al*., 2008; Rabionet *et al*., 2014).

Alterations in ceramides and FFAs are closely associated with the pathophysiology of various dermatoses (Ishikawa *et al*., 2010; Janssens *et al*., 2012; van Smeden *et al*., 2014; Ohno

Open Access **https://doi.org/10.4062/biomolther.2018.214**

Received Nov 4, 2018 **Revised** Dec 7, 2018 **Accepted** Dec 17, 2018
Published Online Feb 8, 2019

***Corresponding Authors**
E-mail: kmlim@ewha.ac.kr (Lim KM), hha@ewha.ac.kr (Ha H), kitaek@yuhs.ac (Nam KT)
Tel: +82-2-3277-3055 (Lim KM), +82-2-3277-4075 (Ha H), +82-2-2228-0754 (Nam KT)
Fax: +82-2-3277-3760 (Lim KM), +82-2-3277-2851 (Ha H), +82-2-2227-8129 (Nam KT)

et al., 2015). Many efforts have been made to understand the implications of alterations in ceramides (Tawada *et al*., 2014) and FFAs (van Smeden *et al*., 2014) for skin diseases and to elucidate the mechanisms underlying those changes (Danso *et al*., 2017). Lines of evidence indicate that the depletion of long-, or very long–chained ceramides and FFAs is linked with impaired skin barrier function (van Smeden *et al*., 2014; Joo *et al*., 2015) and that supplementation with ceramides can improve epidermal homeostasis (Simpson *et al*., 2014; Morifuji *et al*., 2015; Shiba *et al*., 2017). It was also found that the enzymes required to synthesize long-chained FFAs (elongases (ELOVL1, ELOVL4 and ELOVL6)), acylate long FFAs to sphingoid bases [CER synthase 3 (CerS3)], and produce unsaturated FFAs [stearoyl CoA desaturase (SCD)], are altered in atopic dermatitis (Park *et al*., 2012; Danso *et al*., 2017). In the same vein, nuclear receptors governing lipid metabolism and synthesis, such as the liver X receptor (LXR) (Fowler *et al*., 2003) and peroxisome proliferator-activated receptor (PPAR) (Hatano *et al*., 2010) are also involved in the epidermal barrier function and homeostasis (Schmuth *et al*., 2014).

In diabetes mellitus (DM), which causes profound and broad changes in energy metabolism and dyslipidemia (Kumar *et al*., 2013; Sas *et al*., 2016), various skin disorders occur frequently, with a prevalence reaching ~80%, including skin xerosis, itch, infection, and impaired wound healing (Demirseren *et al*., 2014; Macedo *et al*., 2016). Severe forms of diabetic dermopathy also occur, including bullosis diabeticorum, necrobiosis lipoidica diabeticorum, and scleredema diabeticorum (Yosipovitch *et al*., 1998; Quondamatteo, 2014). The frequent occurrence of skin disorders in DM has been explained as an abnormal proliferation and differentiation of keratinocytes and resultant impairment of the skin barrier function (Okano *et al*., 2016). An altered landscape of the skin lipidome has also been suggested to cause the skin disorders of DM (Sakai *et al*., 2003, 2005; Park *et al*., 2011). However, the detailed speciation of the ceramides and FFAs altered by DM and their implications for abnormal skin conditions remain largely unexplored.

Here, we examine the epidermal lipids of db/db mice at 20 weeks of age, which represent Type 2 DM with long-standing hyperglycemia (Quondamatteo, 2014). We used sensitive ultra-performance liquid chromatography tandem mass spectrometry (UPLC-MS/MS) to quantitate 34 ceramides (CER-NP (non-hydroxy fatty acid conjugated to phytosphingosine), CER-NDS (non-hydroxy fatty acid conjugated to dihydrosphingosine), CER-NS (non-hydroxy fatty acid conjugated to sphingosine), and CER-AP (α-hydroxy fatty acid conjugated to phytosphingosine) with varying carbon chain lengths), 14 FFAs (C12, C14, C16, C16:1, C18, C18:1, C18:2, C20, C22, C22:1, C24, C24:1, C26, and C28) and cholesterol (CHOL) in the skin epidermis of db/db mice compared to their normal littermates, db/m mice. In addition, to explore the relationship between the skin and body lipidomes, we examined liver and kidney lipid profiles, the organs most affected by DM. We used principal component analysis (PCA), a metabolomics tool widely used to identify novel biomarkers (Joo *et al*., 2016; Jang *et al*., 2018), to identify global alterations in the lipid profile in DM and to find lipid markers characteristic of DM.

MATERIALS AND METHODS

Materials

An AccQ•Tag Ultra derivatization kit (borate buffer and reagent) and AccQ•Tag Ultra eluents A and B were obtained from Waters (Milford, MA, USA). Ammonium formate, formic acid, and potassium hydroxide were acquired from Sigma-Aldrich (St. Louis, MO, USA). Hydrochloric acid solution and sodium hydroxide were purchased from Daejung (Seoul, Korea). HPLC-grade methanol, ethyl acetate, isopropyl alcohol, and chloroform were purchased from Burdick & Jackson (Muskegon, MI, USA). CHOL and the FFAs (C12, C14, C16, C16:1, C18, C18:1, C18:2, C20, C22, C22:1, C24, C24:1, C26, and C28) were obtained from Sigma-Aldrich. Deuterated FFAs C16-D_3, C20-D_3, and C18:1-D_2 were purchased from Cambridge Isotope Laboratories (Andover, MA, USA). Synthetic CER-NP, CER-NDS, and CER-NS were purchased from Avanti Polar Lipids (Alabaster, AL, USA). Synthetic CER-AP was kindly provided by Evonik (Essen, Germany). 2,2'-dithiodipyridin, 2-picolylamine, and triphenylphosphine were purchased from Sigma-Aldrich. All other reagents used were of the highest grade available. The water used was ultra-pure deionized water (18.2 MΩ•cm) produced using a Milli-Q Gradient system (Millipore, Bedford, MA, USA).

Animal experiments

C57BLKS/J-db/db and age-matched control C57BLKS/J-m+/db mice (five-week-old males, Japan SLC Inc., Hamamatsu, Japan) were housed in a room maintained at 22 ± 2°C with a 12 h dark/12 h light cycle. All animal experiments were conducted according to the Institutional Animal Care and Use Committee of the Ewha Laboratory Animal Genomics Center (IACUC-14-109). Mice were given free access to standard rodent pellets (Purina, Seongnam, Korea). Body weight, fasting blood glucose concentration, and HbA1c level were measured at 8, 14, and 20 weeks. Blood was withdrawn from the cervical vein at the indicated time points; the blood hemoglobin A1c (HbA1c) level was determined using a DCA2000 HbA1c reagent kit (SIEMENS Healthcare Diagnostics, Inc., Tarrytown, NY, USA), and blood glucose was measured using a glucometer (OneTouch Ultra, Johnson & Johnson Co., CA, USA). The moisture and trans-epidermal water loss (TEWL) of each group was measured at the end of the experiments (20 weeks) with a MoistureMeterSC and Vapometer (Delfin Technology, Kuopio, Finland), respectively, after removing hair with an electrical shaver. Liver and skin samples were collected after sacrifice with CO_2.

Histology and tissue sampling

For the histological examination of the skin, 7 mm×1 cm full-thickness skin was excised from the dorsum near the tail and stitched to filter paper before fixing in 10% formalin. For the oil red O staining, skin samples were freshly collected and immediately frozen in Optimal Cutting Temperature (OCT) compound (Tissue TEK®, Sakura Finetek, Tokyo, Japan). Frozen sections were made 8 μm in thickness using a cryostat. Slides were fixed in 70% ethyl-alcohol and then placed in propylene glycol for 5 min. After that, the slides were incubated in 0.7% oil red O (Sigma-Aldrich) solution for 7 min at 60°C. Slides were rinsed with 85% propylene glycol for 3 min and then rinsed with distilled water. Counterstaining was done with Mayer's hematoxylin for 5 min, and then the slides were rinsed

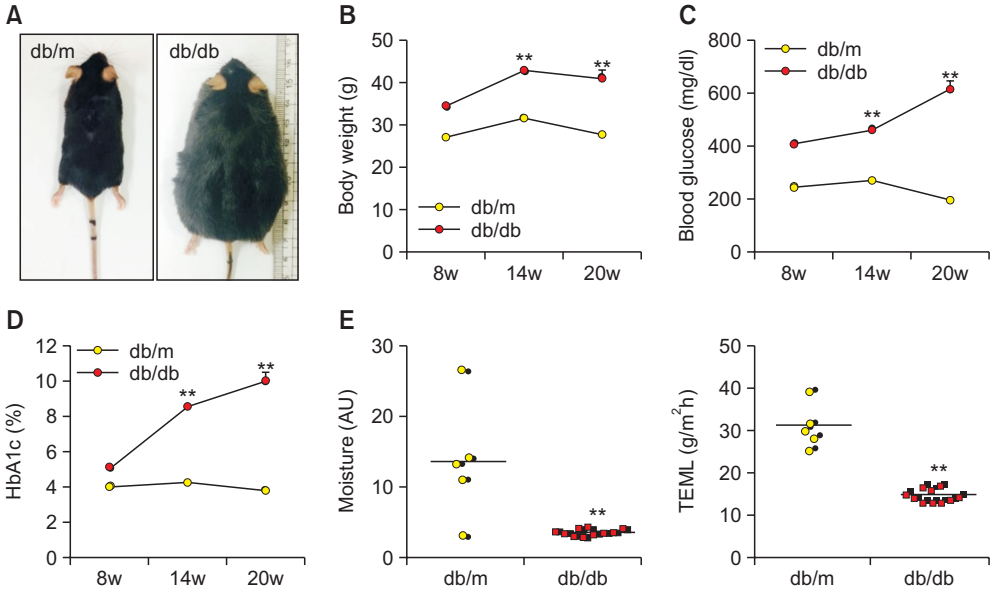

Fig. 1. Macroscopic and functional skin assessment of db/db & db/m mice. (A) Appearance of db/m and db/db mice at 20 weeks of age. The (B) body weight, (C) blood glucose, and (D) HbAc1 of the db/db mice. (E) Moisture and TEWL of db/m and db/db mice. Values are the mean ± SE of 5-10 animals. ** indicates a statistically significant difference from db/m (control) (Student's *t*-test, $p<0.05$, $^{**}p<0.01$).

thoroughly in tap water. Slides were mounted in warmed glycerin jelly solution.

To examine the immunohistochemistry of ceramide, paraffin-embedded skin sections were de-paraffinized and sequentially rehydrated. Antigen retrieval was performed using ph6.0 Target Retrieval solution (DAKO, Glostrup, Denmark) in a pressure cooker for 15 min. After cooling on ice for at least 1 h, sections were incubated in 3% H_2O_2 for 30 min to block endogenous peroxidase. Sections were washed twice with PBS and blocked with a Mouse on Mouse (M.O.M.) kit (Vector Laboratories, Burlingame, CA, USA) overnight at 4°C followed by a protein block (DAKO) for 1 h at room temperature. Then, sections were incubated with anti-ceramide antibody (1:1000, Enzo, Farmingdale, NY, USA) overnight at 4°C. After 3 washes in PBS, sections were incubated in horseradish peroxidase (HRP)-conjugated secondary mouse antibody (DAKO) for 15 min at room temperature. For immunohistochemistry experiments, diaminobenzidine (DAB) (DAKO) was used for antibody development, and Mayer's hematoxylin (DAKO) was used for counter staining.

To prepare the epidermal sheet for lipid sampling, the skin was disinfected with povidone and treated in 0.25% EDTA-free trypsin for digestion overnight. The dermis was removed with tweezers to collect the epidermis. To prepare the liver tissue sample, the liver was perfused with PBS, and 100 mg tissue was collected from the same lobe in each animal. For the kidney samples, about 50 mg of kidney cortex was collected.

Analysis of lipids

Lipid extraction and sample preparation: Epidermal sheets or tissues were minced into small pieces in ice-cold 0.1% ammonium acetate followed by homogenization in a Precellys 24 (6500 rpm 1×30s, Bertin Instrument, Montigny-le-Bretonneux, France). Methanol (1.5 mL) was added to a 200 μL sample aliquot, which was placed into a glass tube with a Teflon-lined cap, and the tube was vortexed. Then, 5 mL of methyl-tert-butyl ether (MTBE) was added, and the mixture was incubated for 1 h at room temperature in a shaker. Phase separation was induced by adding 1.25 mL of MS-grade water. After 10 min of incubation at room temperature, the sample was centrifuged at 1,000 g for 10 min. The top 4 mL (organic phase) was collected. The solvent was volatilized using a Speedvac (EZ-2 Plus, Genevac, Ipswich, UK). Each 4 mL of the filtrate was united and evaporated to dryness using a Speedvac at 40°C. The residues (extractable lipids) were reconstituted in 500 μL of chloroform–methanol 2:1 (v/v) for analysis by UPLC-MS/MS. A standard stock solution of individual lipids (ca. 1 mg/mL) was prepared by dissolving specific amounts of authentic standards in chloroform-methanol (1:1, v/v) and then storing it at –20°C. The working standard solutions of the lipid mixtures were serially diluted with chloroform-methanol (2:1, v/v) to obtain the concentrations needed for calibration curve standards. FFAs were quantified through derivatization according to a method previously described (Joo *et al*., 2013).

UPLC-MS/MS: The chromatographic separation was carried out using an ACQUITY UPLC system (Waters, Manchester, UK) equipped with an ACQUITY UPLC BEH C18 column (1.7 μm, 2.1×50 mm). The column temperature and autosampler tray temperature were maintained at 55°C and 4°C, respectively. The mobile phase for the CER (CER-NDS, CER-NS, CER-AP, CER-NP) and FFA analyses consisted of methanol: water=1:1 (v/v, 2 mM ammonium formate and 0.1% formic acid, solvent A) and methanol: isopropyl alcohol=6:4 (v/v, 2 mM ammonium formate and 0.1% formic acid, solvent B). Gradient elution was initiated with 20% B (50% B for the CER analysis) for 0.5 min and changed to 100% B in 2 min. The isocratic elution with 100% B was kept for 5 min and then returned to 20% B (50% B for CERs analysis) in 6.5 min. The total run time was 6.5 min. The flow rate was 0.3 mL/min, and the injection volume was 2 μL.

The UPLC-MS/MS analysis was performed using a Waters Micromass Quattro Premier XE triple quadrupole mass spec-

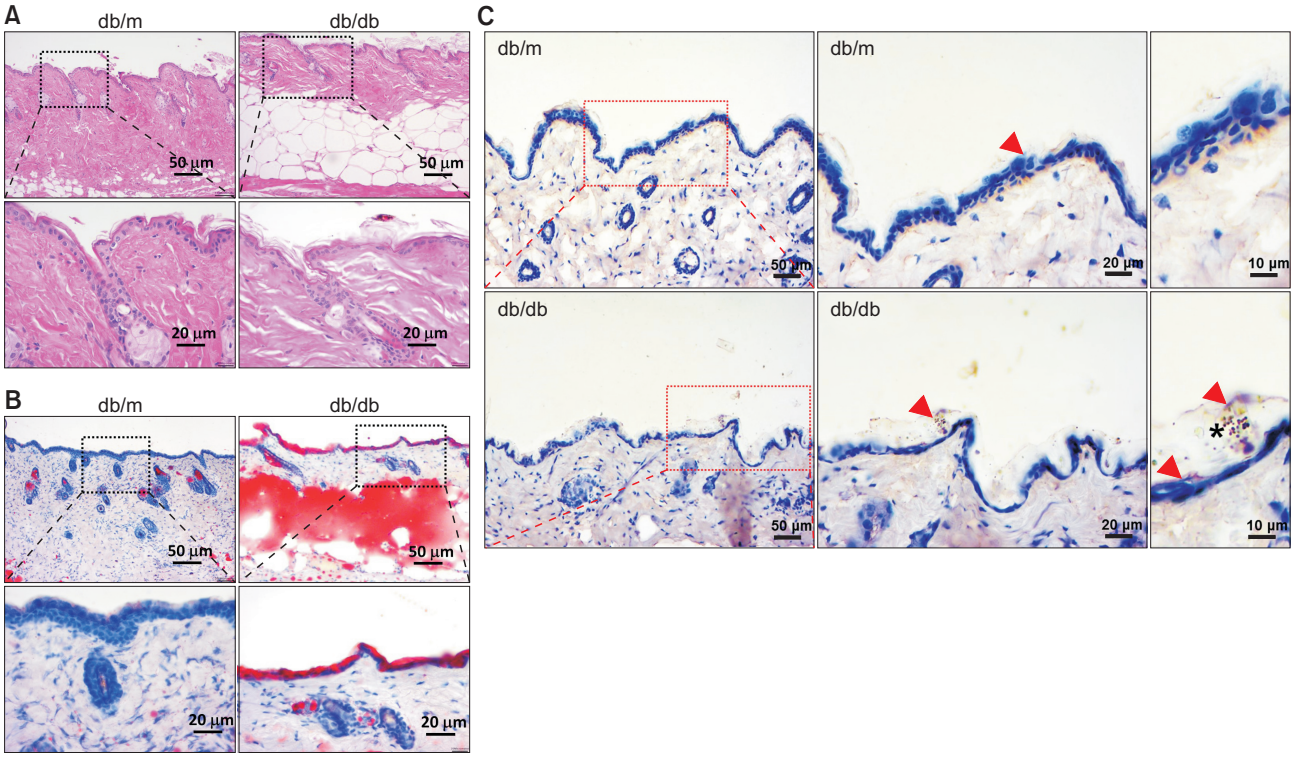

Fig. 2. Histological appearance of the skin of db/db and db/m mice. (A) H&E and (B) oil-red O staining of the skin of db/db and db/m mice. (C) Immunohistochemical staining for ceramides in the skin of db/db and db/m mice. Red arrows indicate a representative signal for ceramides in the stratum corneum of db/m and db/db mice.

trometer. The ESI-MS spectra were acquired in the positive ion multiple reaction monitoring (MRM) mode with a capillary voltage of 3.5 kV, source temperature of 120°C, desolvation temperature of 350°C, desolvation gas flow rate of 750 L/h, and cone gas flow rate of 50 L/h. The optimum cone voltages for the FFAs and CERs were set to 20 and 25 eV, respectively. The collision energy for the MRM mode was optimized for each analyte.

The cholesterol analysis was performed with a gradient elution of water (solvent A) and acetonitrile (solvent B). The gradient elution was initiated with 85% B for 0.5 min and changed to 100% B in 1.5 min. The isocratic elution with 100% B was kept for 3.5 min and then returned to 85% B in 5.0 min. The flow rate was 0.4 mL/min, and the injection volume was 2 μL.

The APCI-MS spectra were acquired in positive ion mode with an APCI corona current of 4.0 mA, a source temperature of 120°C, desolvation temperature of 400°C, and desolvation gas flow rate of 500 L/h. The optimum cone voltage was 35 V. The collision energy for the MRM mode was optimized to 6 eV (*m/z* 369.2>369.2). We controlled the data acquisition and process with a MassLynx Version 4.1 (Waters).

RNA isolation

Liver and skin samples were lysed using Trizol (Invitrogen, CA, USA). After the addition of chloroform, samples were centrifuged at 12,000 rpm for 10 min. The aqueous phase was mixed with isopropanol, and RNA pellets were collected by centrifugation (12,000 rpm, 15 min, 4°C). The RNA pellets were washed with 70% ethanol and dissolved in RNase-free, DEPC (diethyl pyrocarbonate)-treated water (Waltham, MA, USA). The RNA yield was estimated by determining the optical density at 260 nm with a NanoDrop 1000 spectrophotometer (NanoDrop Technologies, INC., Wilmington, DE, USA).

Real-time PCR

The relative mRNA expression levels were measured using quantitative real-time PCR. cDNA was synthesized from 1250 ng of total RNA with oligo (dT) (Bioelpis, Seoul, Korea). SYBR Green PCR master mix and a StepOnePlusTM real-time PCR machine (Applied Biosystems, Warrington, UK) were used in each reaction. The sequence of primers was as follows: forward LXRα, 5′-ACT TTG CCA AAC AGC TCC CT-3′; reverse LXRα, 5′- AAG GTG ATG CTC TCA CTG CC-3′; forward LXRβ, 5′-TGG ACG ATG CAG AGT ATG CC-3′; reverse LXRβ, 5′-TCC TCG TGT AGG AGA GGA GC-3′; forward PPARγ, 5′-TGA ACG TGA AGC CCA TCG AG-3′; reverse PPARγ, 5′-CGA TCT GCC TGA GGT CTG TC-3′; forward Elovl6, 5′-CTG GAT GCA GCA TGA CAA CG-3′; reverse Elovl6, 5′-GCC GAT GTA GGC CTC AAA GA-3′; forward Elovl1, 5′-TAC CCC ATC ATC ATC CAC CT-3′; reverse Elovl1, 5′-GGA GCT CCA TTT TGC TGA AC-3′; forward Elovl4, 5′-GTC TCT CTA CAC CGA CTG CC-3′; reverse Elovl4, 5′-CCG GTT TTT GAC TGC TTC GG-3′; forward FAS, 5′-AGC TAC CGG GCA AAG ATG AC-3′; reverse FAS, 5′-CCC GAT CTT CCA GGC TCT TC-3′; forward SCD, 5′-AGC CTG TTC GTT AGC ACC TT-3′; reverse SCD, 5′-CCA GGA TAT TCT CCC GGG ATT G-3’. Cycling parameters were 51°C for 2 min, 95°C for 10 min, 40 cycles of 95°C for 15 s, and 51°C for 1 min.

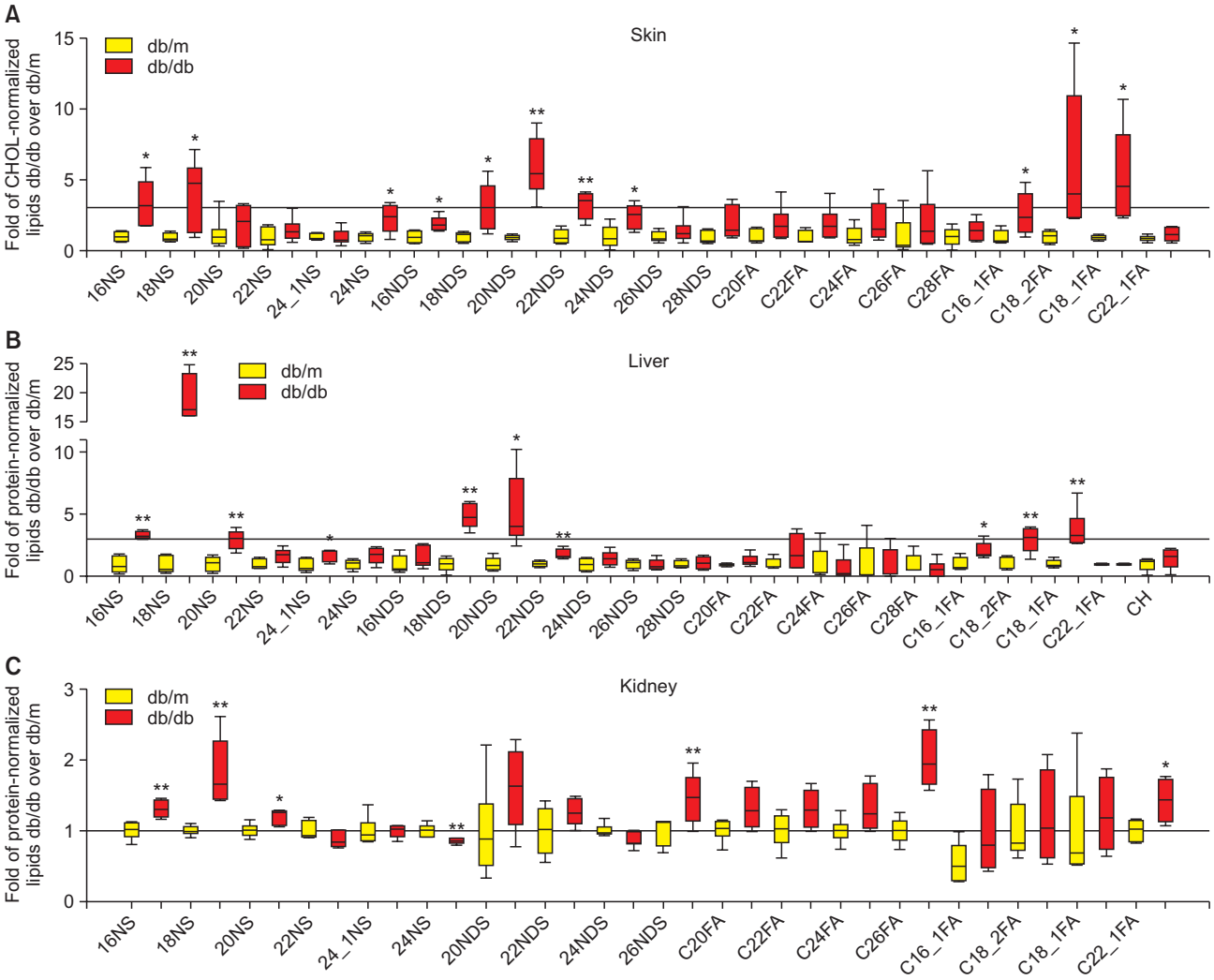

Fig. 3. Ceramides and free fatty acids in the skin, liver, and kidneys of db/db mice compared to db/m mice. (A) Cholesterol-normalized lipid abundance in the skin epidermis of db/db mice (as fold of that in db/m mice). Protein-normalized lipids in the (B) liver and (C) kidney. Values are presented as a box whisker plot. The ends of the box are the upper and lower quartiles, so the box spans the interquartile range. The median is marked by a vertical line inside the box. The whiskers are the two lines outside the box and extend to the highest and lowest observations (n=5-6. *p<0.05, **p<0.01).

Statistical analysis

Data are presented as the mean ± SD. PCA for the lipid profiles were done using SIMCA-P+ (v12.0 version, Umetrics, Umea, Sweden). Data were analyzed by Student's t-test to identify statistically significant differences from the control group. Significance was acknowledged when p<0.05.

RESULTS

Reduced skin hydration, trans-epidermal water loss, and altered skin lipid profiles in db/db mice, a Type 2 diabetes mellitus model

DM was well-established in the db/db mice from the age of 14 weeks, as determined by high body weights (Fig. 1A, 1B), evident hyperglycemia (Fig. 1C), and significantly increased levels of hemoglobin A1c (HbAc1) (Fig. 1D). At the age of 20 weeks, HbAc1 was 2.6 fold higher than in the db/m mice, and blood glucose exceeded the control by >3.0 fold, reflecting a chronic stage of severe hyperglycemia. At 20 weeks, skin moisture and TEWL were significantly lower in the db/db mice than in the db/m mice (Fig. 1E), suggesting the impairment of epidermal homeostasis. Histological examination revealed that the skin of the db/db mice was markedly thickened (Fig. 2A), which was largely attributable to an increased subcutaneous fat bed. In contrast, the epidermis and dermis of the db/db mice was rather compressed and had a flaky appearance. Lipid-specific oil-red O staining of the skin suggested a profound increase in the lipids in the epidermis and subcutis of the db/db mice (Fig. 2B). The immunohistochemical analysis of ceramide using ceramide-specific antibody revealed that the distribution and content of ceramides were also substantially altered in the skin epidermis of the db/db mice (Fig. 2C).

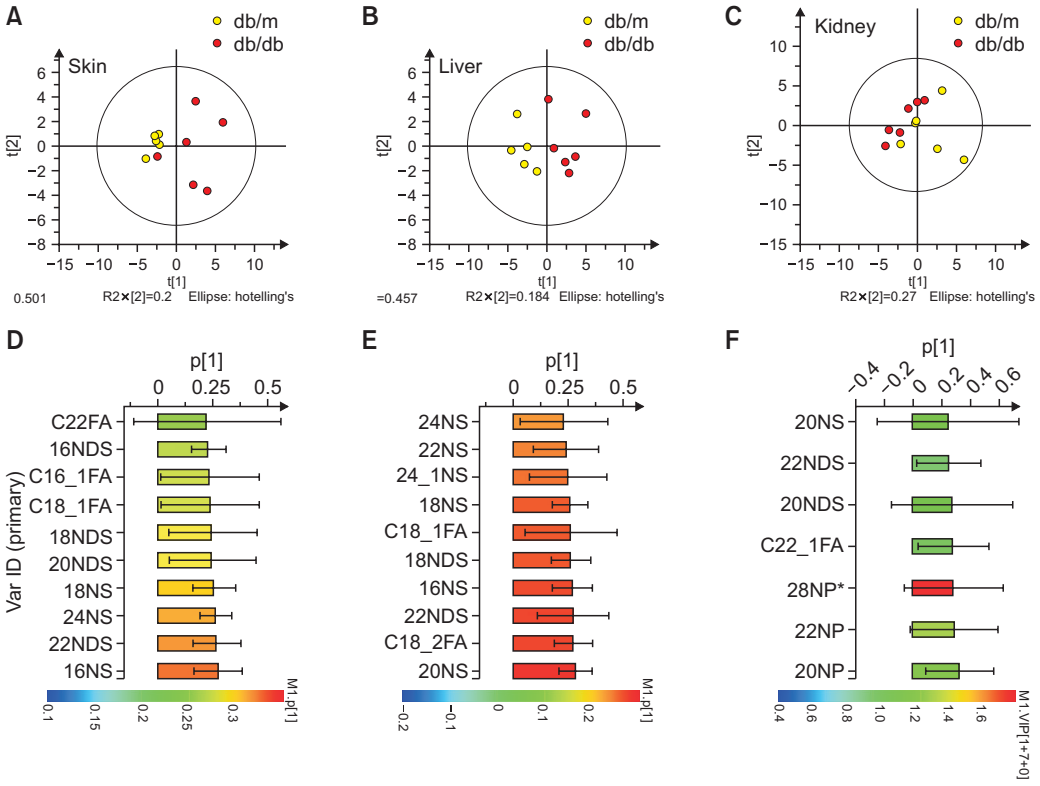

Fig. 4. Principal component analysis for lipids in db/m and db/db mice. PCA scatter plot for lipids of the (A) skin, (B) liver, and (C) kidney. X axis represents principal component 1 (t[1]), and the Y axis represents principal component 2 (t[2]). The ellipse error shows the 95% confidence interval. A loading plot is presented for principal component 1 (t[1]) for the lipids of the (D) skin, (E) liver, and (F) kidney.

Higher levels of medium-chained ceramides and FFAs in the skin epidermis, liver, and kidneys of the db/db mice

Ceramides, FFAs, and CHOL constitute the major skin epidermal lipid classes. Their composition significantly affects epidermal homeostasis, and their alteration is closely linked with skin diseases (Li *et al*., 2016). The quantitation of ceramides, saturated and unsaturated FFAs, and CHOL in the skin epidermis, the liver, and the kidneys revealed that most ceramides and FFAs were significantly higher in the db/db mice than in the db/m mice (Fig. 3A-3C). These patterns became evident and statistically significant when the skin lipids were normalized with CHOL (Joo *et al*., 2015) and those of the liver and kidney with protein content. Specifically, ceramides with medium-length chains (16NS, 18NS, 18NDS, 20NDS, and 22NDS), and unsaturated C18 FFAs (C18:2FA and C18:1FA) were ≥3 fold higher in the skin epidermis, whereas in the liver, 16NS, 18NS, 20NS, 18NDS, 20NDS, C16:1FA, C18:2FA, and C18:1FA were higher (Fig. 3A, 3B). The alteration in the amount of ceramides and FFAs was markedly attenuated in the kidney, but similarly, 16NS, 18NS, 26NDS, and C26FA were more plentiful in the db/db mice than in the db/m mice. The PCA for the lipid changes further indicated that db/db mice could be differentiated from db/m by the lipids in their skin and liver (Fig. 4A, 4B) and to a lesser extent their kidney (Fig. 4C). Loading plots drawn in ascending order revealed that 16NS, 22NDS, 24NS, and 18NS were the key differentiators of db/db vs. db/m mice in the skin epidermis, whereas in the liver, 20NS, C18:2FA, 22NDS, and 16NS were distinctive (Fig. 4D, 4E). In the kidney, the variations in loadings (i.e., confidence interval) was large (Fig. 4F), indicating that the differences in the lipid content between db/db and db/m mice were minute.

Increased gene expression involved in lipid synthesis in the liver and skin of db/db mice

To investigate the mechanism underlying the alteration of epidermal and liver lipids in db/db mice, we evaluated the expression of genes associated with lipid synthesis reported previously (Rabionet *et al*., 2014). Nuclear receptors related to lipid metabolism (LXR/β and PPAR) and lipid synthesizing enzymes [fatty acid synthase (FAS), elongases (Elovl1, 4 and 6), and stearoyl-CoA desaturase (SCD)] were examined for their expression using qPCR. As shown in Fig. 5A and 5B, significant increases in the expression of LXRβ, PPARγ, Elovl6, Elovl1, Elovl4, and SCD were noted in the skin of db/db mice compared with db/m mice, whereas LXRα/β, PPARγ, Elovl6, FAS, and SCD were significantly higher in the livers of db/db mice, indicating a profound change in both lipid metabolism and synthesis in both the skin and livers of db/db mice.

DISCUSSION

In this study, we have demonstrated that db/db mice at the age of 20 weeks (representing longstanding, chronic hyperglycemia) exhibited reduced skin moisture and TEWL (Fig. 1A-1E) compared to controls. Of note, ceramides and FFAs with medium chains were highly enriched in the skin epidermis of db/db mice, and those alteration patterns were repeated in

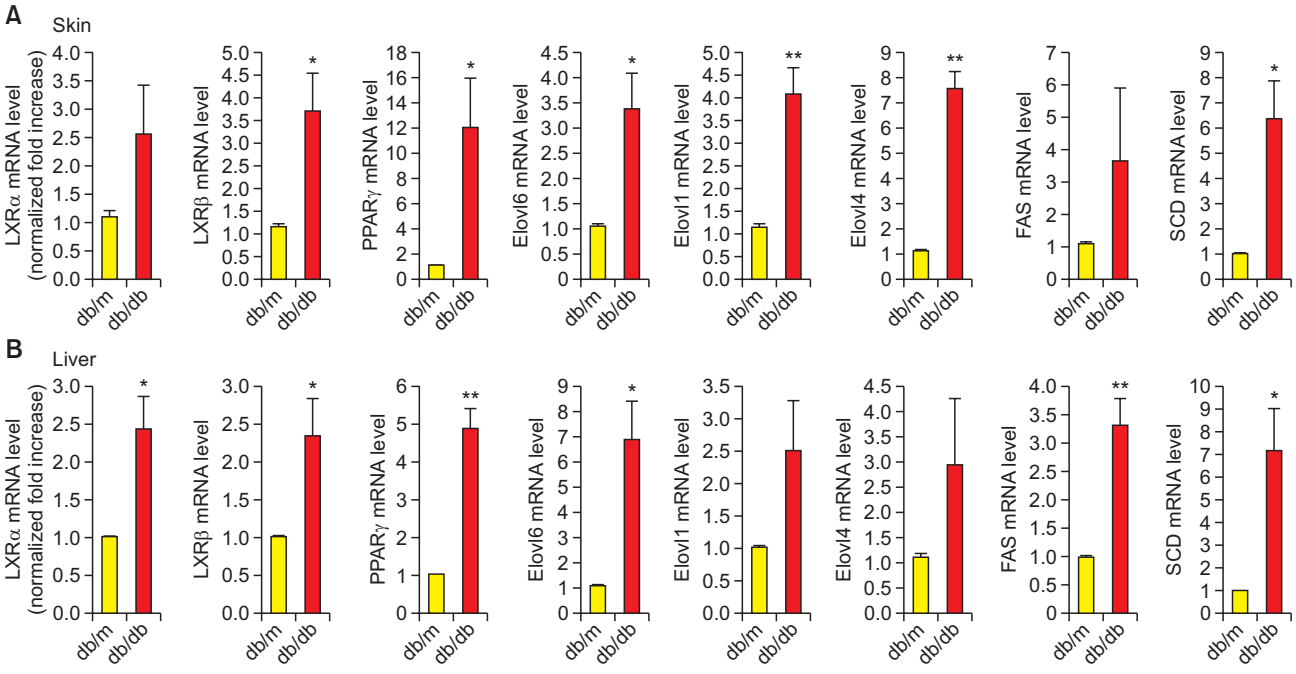

Fig. 5. Expression profiles for enzymes or molecules related to lipid metabolism. The mRNA expression levels in the (A) skin and (B) liver of db/m and db/db mice were determined using real-time PCR. The analyzed genes were LXRα (liver X receptor α, NR1H3), LXRβ (liver X receptor β, NR1H2), PPARγ (peroxisome proliferator activated receptor gamma), Elovl6 (elongation of long chain fatty acids 6), Elovl1 (elongation of long chain fatty acids 1), Elovl4 (elongation of long chain fatty acids 4), FAS (fatty acid synthase), and SCD (stearoyl-CoA desaturase). Values were normalized to glyceraldehyde 3-phosphate dehydrogenase (GAPDH) level. Data are presented as the mean ± SE (n=3, *p<0.05 and **p<0.01).

the liver (Fig. 3A, 3B), whereas in the kidney, the difference from db/m mice was markedly attenuated (Fig. 3C), suggesting the existence of cross-talk in lipid synthesis and metabolism between the epidermis and the liver.

In this study, we demonstrated that db/db mice show significantly reduced skin hydration and TEWL compared to db/m mice (skin moisture, 3.6 ± 0.18 (n=10) vs. 13.6 ± 3.8 (n=5); TEWL 14.87 ± 0.5944 (n=10) vs. 30.82 ± 2.481 (n=5), t-test, p<0.05), indicating that epidermal homeostasis might be disrupted in DM. Reduced skin hydration in DM has been demonstrated in both DM patients (Sakai *et al*., 2005) and experimental DM models [the Otsuka Long-Evans Tokushima Fatty (OLETF) rat (Park *et al*., 2011) and streptozotocin or alloxan-induced DM (Sakai *et al*., 2003)], in line with our findings. In addition, Han and Park recently demonstrated that longstanding hyperglycemia resulted in lower TEWL in the extremities of DM patients (Han and Park, 2017), further supporting our finding that longstanding DM can lead to impaired epidermal homeostasis.

Ceramides and FFAs with medium chains were enriched in the skin epidermis (Fig. 3A) of db/db mice, and those patterns were similarly observed in the liver (Fig. 3B). Interestingly, the alteration pattern of lipids in DM was distinct from that observed in skin affected by atopic dermatitis (AD), a representative inflammatory dermatose with xerosis. In AD, asymmetric alteration of ceramides across chain lengths was observed, and ceramides with short chains (≤C22) increased in the epidermis, whereas ceramides with medium or long chains (≥C24) decreased significantly (Joo *et al*., 2015). Although the total amount of lipids in the epidermis of db/db mice increased, ceramides with short chains (≤C24) increased whereas ceramides with long chains (>C24) were not significantly altered, resulting in a relative abundance of the shorter chains. The proper ratio and distribution of ceramides and FFAs across varying chain lengths, as well as their overall amounts, are important for maintaining epidermal homeostasis (Mojumdar *et al*., 2014) and skin barrier function (Oguri *et al*., 2014). Whereas short-chain lipids are important for membrane fluidity, long-chained ceramides have a higher stacking capacity and are pivotal in constructing a robust lamella structure (Ramos and Lafleur, 2015). The disproportionately high ratios of short ceramides in DM could negatively affect the skin barrier function by tipping the balance of lipids toward shorter chains, leading to weaker stacking capacity and higher fluidity; however further studies are needed to elucidate that finding.

In addition to hyperglycemia, DM causes dyslipidemia, although its extent and patterns vary across tissues and with disease severity (Sas *et al*., 2016). Previously, it was shown that streptozotocin-induced DM led to increased phospholipids and FFAs in the blood and livers of mice (Kumar *et al*., 2013). Specifically, C18:1FA and ceramides with short chains were highly enriched in the liver. However, lipid profiles in the skin epidermis remain controversial. Sakai *et al*. (2003) reported that streptozotocin-treated mice showed overall increases in ceramides and FFAs of the epidermis, whereas Park *et al*. demonstrated that the OLETF rat model exhibited reduced FFAs without changes in ceramides (Park *et al*., 2011), indicating that physiological changes and ambient conditions affect skin lipids. By using db/db mice at the age of 20 weeks to represent severe and chronic hyperglycemia, our study dem-

onstrated that ceramides and FFAs with short chains might be disproportionately enriched in chronic hyperglycemia.

Interestingly, the lipid profiles of both db/db and db/m mice were similar in the skin and livers of individual animals, suggesting cross-talk between the skin and liver in lipid synthesis and metabolism. The PCA revealed a remarkable difference in the lipids of both the skin and the liver between db/db and db/m mice (Fig. 4A-4F). Of note, the lipids of marked distinction in both tissues largely overlapped, further supporting the close relationship between the skin and the liver in lipid synthesis. Indeed, the liver is known as a central organ for synthesizing and distributing lipids to peripheral tissues, and coordinated changes in certain lipids occur between the skin and the liver in disease states (Miyazaki *et al*., 2005).

In addition, we demonstrated that the *de novo* synthesis of lipids in the skin in DM might be altered in the same pattern seen in the liver. We found that molecules related to lipid metabolism and synthesis (LXRα (NR1H3), LXRβ (NR1H2), PPARγ, Elovl1, 4, and 6, FAS, and SCD) were upregulated in the skin and livers of db/db mice, suggesting that lipid synthesis is stimulated both peripherally and centrally in db/db mice. LXRα/ play central roles in lipid metabolism and cholesterol homeostasis, which regulate the expression of elongases (Park *et al*., 2012), apolipoprotein E, and ATP-binding cassette protein A1 (Lee *et al*., 2013). Importantly, the role of LXRα/β has been suggested in skin diseases such as AD (Czarnowicki *et al*., 2018), psoriasis (Gupta *et al*., 2010), and vitiligo (Kumar *et al*., 2010), so the alteration of LXR might also be involved in DM skin disorders. PPARγ is critical to epidermal barrier function, regulating lipid uptake and adipogenesis as well as epidermal marker expression (Gupta *et al*., 2015). Indeed, dysregulation of LXR and PPARγ could be involved in abnormal epidermal homeostasis (Elias, 2005), and their activation promotes the expression of genes related to lipid synthesis and transport. Elongases are key to the synthesis of very long–chain fatty acids, mediating the condensation of acyl-CoA and malonyl-Coa to produce 3-ketoacyl-CoA (Jakobsson *et al*., 2006). FAS and SCD also play critical roles in the synthesis of fatty acids, producing a saturated fatty acid, palmitic acid (C16:0), from acetyl-CoA and malonyl-CoA (Smith *et al*., 2003) and forming monounsaturated fatty acids (Paton and Ntambi, 2009) respectively. Elongases, FAS, and SCD also receive positive regulation from lipid metabolites and nuclear receptors, including LXR and PPARγ, which explains how their higher expression in db/db mice could contribute to the enrichment of lipids in the skin and liver.

In conclusion, we have demonstrated that remarkable changes occur in the lipid profiles of the skin epidermis of db/db mice, a Type 2 DM model, and that those changes coincide with changes in the liver and kidneys. The alteration of these lipids, which are critical to the normal homeostasis of the skin epidermis, could explain, at least in part, the abnormal skin barrier, hydration, and compromised defense against infection seen in DM patients.

CONFLICT OF INTEREST

None.

ACKNOWLEDGMENTS

This work was supported by the National Research Foundation of Korea (Grant No. 2016R1A2B4006575 and 2017R1A6A3A11034070) and the Korea government (MSIT) (2018R1A5A2025286).

REFERENCES

Breiden, B. and Sandhoff, K. (2014) The role of sphingolipid metabolism in cutaneous permeability barrier formation. *Biochim. Biophys. Acta* **1841**, 441-452.

Czarnowicki, T., Dohlman, A. B., Malik, K., Antonini, D., Bissonnette, R., Chan, T. C., Zhou, L., Wen, H. C., Estrada, Y., Xu, H., Bryson, C., Shen, J., Lala, D., Ma'ayan, A., McGeehan, G., Gregg, R. and Guttman-Yassky, E. (2018) Effect of short-term liver X receptor activation on epidermal barrier features in mild to moderate atopic dermatitis: A randomized controlled trial. *Ann. Allergy. Asthma. Immunol.* **120**, 631-640.e11.

Danso, M. O., Boiten, W., van Drongelen, V., Gmelig, K. M., Gooris, G., El Ghalbzouri, A., Absalah, S., Vreeken, R., Kezic, S., van Smeden, J., Lavrijsen, A. P. M. and Bouwstra, J. A. (2017) Altered expression of epidermal lipid bio-synthesis enzymes in atopic dermatitis skin is accompanied by changes in stratum corneum lipid composition. *J. Dermatol. Sci.* **88**, 57-66.

Demirseren, D. D., Emre, S., Akoglu, G., Arpacı, D., Arman, A., Metin, A. and Cakır, B. (2014) Relationship between skin diseases and extracutaneous complications of diabetes mellitus: clinical analysis of 750 patients. *Am. J. Clin. Dermatol.* **15**, 65-70.

Elias, P. M. (2005) Stratum corneum defensive functions: an integrated view. *J. Invest. Dermatol.* **125**, 183-200.

Fowler, A. J., Sheu, M. Y., Schmuth, M., Kao, J., Fluhr, J. W., Rhein, L., Collins, J. L., Willson, T. M., Mangelsdorf, D. J. and Elias, P. M. (2003) Liver X receptor activators display anti-inflammatory activity in irritant and allergic contact dermatitis models: liver-X-receptor-specific inhibition of inflammation and primary cytokine production. *J. Invest. Dermatol.* **120**, 246-255.

Gupta, D. S., Kaul, D., Kanwar, A. J. and Parsad, D. (2010) Psoriasis: crucial role of LXR-alpha RNomics. *Genes Immun.* **11**, 37-44.

Gupta, M., Mahajan, V. K., Mehta, K. S., Chauhan, P. S. and Rawat, R. (2015) Peroxisome proliferator-activated receptors (PPARs) and PPAR agonists: the 'future' in dermatology therapeutics? *Arch. Dermatol. Res.* **307**, 767-780.

Han, S. H. and Park, J. W. (2017) Diabetic and sympathetic influences on the water permeability barrier function of human skin as measured using transepidermal water loss: a case-control study. *Medicine (Baltimore)* **96**, e8611.

Hatano, Y., Man, M.-Q., Uchida, Y., Crumrine, D., Mauro, T. M., Feingold, K. R., Elias, P. M. and Holleran, W. M. (2010) Murine atopic dermatitis responds to peroxisome proliferator-activated receptors α and β/δ (but not γ) and liver X receptor activators. *J. Allergy Clin. Immunol.* **125**, 160-169. e5.

Ishikawa, J., Narita, H., Kondo, N., Hotta, M., Takagi, Y., Masukawa, Y., Kitahara, T., Takema, Y., Koyano, S., Yamazaki, S. and Hatamochi, A. (2010) Changes in the ceramide profile of atopic dermatitis patients. *J. Invest. Dermatol.* **130**, 2511-2514.

Jakobsson, A., Westerberg, R. and Jacobsson, A. (2006) Fatty acid elongases in mammals: their regulation and roles in metabolism. *Prog. Lipid Res.* **45**, 237-249.

Jang, H. J., Lee, J. D., Jeon, H. S., Kim, A. R., Kim, S., Lee, H. S. and Kim, K. B. (2018) Metabolic profiling of eccentric exercise-induced muscle damage in human urine. *Toxicol. Res.* **34**, 199-210.

Janssens, M., van Smeden, J., Gooris, G. S., Bras, W., Portale, G., Caspers, P. J., Vreeken, R. J., Hankemeier, T., Kezic, S., Wolterbeek, R., Lavrijsen, A. P. and Bouwstra, J. A. (2012) Increase in short-chain ceramides correlates with an altered lipid organization and decreased barrier function in atopic eczema patients. *J. Lipid Res.* **53**, 2755-2766.

Joo, K. M., Choi, D., Park, Y. H., Yi, C. G., Jeong, H. J., Cho, J. C. and

Lim, K. M. (2013) A rapid and highly sensitive UPLC-MS/MS method using pre-column derivatization with 2-picolylamine for intravenous and percutaneous pharmacokinetics of valproic acid in rats. *J. Chromatogr. B Analyt. Technol. Biomed. Life Sci.* **938**, 35-42.

Joo, K. M., Hwang, J. H., Bae, S., Nahm, D. H., Park, H. S., Ye, Y. M. and Lim, K. M. (2015) Relationship of ceramide-, and free fatty acid-cholesterol ratios in the stratum corneum with skin barrier function of normal, atopic dermatitis lesional and non-lesional skins. *J. Dermatol. Sci.* **77**, 71-74.

Joo, K. M., Kim, A. R., Kim, S. N., Kim, B. M., Lee, H. K., Bae, S., Lee, J. H. and Lim, K. M. (2016) Metabolomic analysis of amino acids and lipids in human hair altered by dyeing, perming and bleaching. *Exp. Dermatol.* **25**, 729-731.

Joo, K. M., Nam, G. W., Park, S. Y., Han, J. Y., Jeong, H. J., Lee, S. Y., Kim, H. K. and Lim, K. M. (2010) Relationship between cutaneous barrier function and ceramide species in human stratum corneum. *J. Dermatol. Sci.* **60**, 47-50.

Kendall, A. C. and Nicolaou, A. (2013) Bioactive lipid mediators in skin inflammation and immunity. *Prog. Lipid Res.* **52**, 141-164.

Kendall, A. C., Pilkington, S. M., Massey, K. A., Sassano, G., Rhodes, L. E. and Nicolaou, A. (2015) Distribution of bioactive lipid mediators in human skin. *J. Invest. Dermatol.* **135**, 1510-1520.

Kumar, R., Parsad, D., Kaul, D. and Kanwar, A. J. (2010) Liver X receptor expression in human melanocytes, does it have a role in the pathogenesis of vitiligo? *Exp. Dermatol.* **19**, 62-64.

Kumar, R. N., Sundaram, R., Shanthi, P. and Sachdanandam, P. (2013) Protective role of 20-OH ecdysone on lipid profile and tissue fatty acid changes in streptozotocin induced diabetic rats. *Eur. J. Pharmacol.* **698**, 489-498.

Lee, C. S., Park, M., Han, J., Lee, J. H., Bae, I. H., Choi, H., Son, E. D., Park, Y. H. and Lim, K. M. (2013) Liver X receptor activation inhibits melanogenesis through the acceleration of ERK-mediated MITF degradation. *J. Invest. Dermatol.* **133**, 1063-1071.

Li, S., Ganguli-Indra, G. and Indra, A. K. (2016) Lipidomic analysis of epidermal lipids: a tool to predict progression of inflammatory skin disease in humans. *Expert Rev. Proteomics* **13**, 451-456.

Macedo, G. M. C., Nunes, S. and Barreto, T. (2016) Skin disorders in diabetes mellitus: an epidemiology and physiopathology review. *Diabetol. Metab. Syndr.* **8**, 63.

Masukawa, Y., Narita, H., Shimizu, E., Kondo, N., Sugai, Y., Oba, T., Homma, R., Ishikawa, J., Takagi, Y. and Kitahara, T. (2008) Characterization of overall ceramide species in human stratum corneum. *J. Lipid Res.* **49**, 1466-1476.

Miyazaki, M., Dobrzyn, A., Elias, P. M. and Ntambi, J. M. (2005) Stearoyl-CoA desaturase-2 gene expression is required for lipid synthesis during early skin and liver development. *Proc. Natl. Acad. Sci. U.S.A.* **102**, 12501-12506.

Mojumdar, E. H., Kariman, Z., van Kerckhove, L., Gooris, G. S. and Bouwstra, J. A. (2014) The role of ceramide chain length distribution on the barrier properties of the skin lipid membranes. *Biochim. Biophys. Acta* **1838**, 2473-2483.

Morifuji, M., Oba, C., Ichikawa, S., Ito, K., Kawahata, K., Asami, Y., Ikegami, S., Itoh, H. and Sugawara, T. (2015) A novel mechanism for improvement of dry skin by dietary milk phospholipids: Effect on epidermal covalently bound ceramides and skin inflammation in hairless mice. *J. Dermatol. Sci.* **78**, 224-231.

Oguri, M., Gooris, G. S., Bito, K. and Bouwstra, J. A. (2014) The effect of the chain length distribution of free fatty acids on the mixing properties of stratum corneum model membranes. *Biochim. Biophys. Acta* **1838**, 1851-1861.

Ohno, Y., Nakamichi, S., Ohkuni, A., Kamiyama, N., Naoe, A., Tsujimura, H., Yokose, U., Sugiura, K., Ishikawa, J., Akiyama, M. and Kihara, A. (2015) Essential role of the cytochrome P450 CYP4F22 in the production of acylceramide, the key lipid for skin permeability barrier formation. *Proc. Natl. Acad. Sci. U.S.A.* **112**, 7707-7712.

Okano, J., Kojima, H., Katagi, M., Nakagawa, T., Nakae, Y., Terashima, T., Kurakane, T., Kubota, M., Maegawa, H. and Udagawa, J. (2016) Hyperglycemia induces skin barrier dysfunctions with impairment of epidermal integrity in non-wounded skin of type 1 diabetic mice. *PLoS ONE* **11**, e0166215.

Park, H. Y., Kim, J. H., Jung, M., Chung, C. H., Hasham, R., Park, C. S. and Choi, E. H. (2011) A long-standing hyperglycaemic condition impairs skin barrier by accelerating skin ageing process. *Exp. Dermatol.* **20**, 969-974.

Park, Y. H., Jang, W. H., Seo, J. A., Park, M., Lee, T. R., Park, Y. H., Kim, D. K. and Lim, K. M. (2012) Decrease of ceramides with very long-chain fatty acids and downregulation of elongases in a murine atopic dermatitis model. *J. Invest. Dermatol.* **132**, 476-479.

Paton, C. M. and Ntambi, J. M. (2009) Biochemical and physiological function of stearoyl-CoA desaturase. *Am. J. Physiol. Endocrinol. Metab.* **297**, E28-E37.

Quondamatteo, F. (2014) Skin and diabetes mellitus: what do we know? *Cell Tissue Res.* **355**, 1-21.

Rabionet, M., Gorgas, K. and Sandhoff, R. (2014) Ceramide synthesis in the epidermis. *Biochim. Biophys. Acta* **1841**, 422-434.

Ramos, A. P. and Lafleur, M. (2015) Chain length of free fatty acids influences the phase behavior of stratum corneum model membranes. *Langmuir* **31**, 11621-11629.

Sakai, S., Endo, Y., Ozawa, N., Sugawara, T., Kusaka, A., Sayo, T., Inoue, S. and Tagami, H. (2003) Characteristics of the epidermis and stratum corneum of hairless mice with experimentally induced diabetes mellitus. *J. Invest. Dermatol.* **120**, 79-85.

Sakai, S., Kikuchi, K., Satoh, J., Tagami, H. and Inoue, S. (2005) Functional properties of the stratum corneum in patients with diabetes mellitus: similarities to senile xerosis. *Br. J. Dermatol.* **153**, 319-323.

Sas, K. M., Kayampilly, P., Byun, J., Nair, V., Hinder, L. M., Hur, J., Zhang, H., Lin, C., Qi, N. R. and Michailidis, G. (2016) Tissue-specific metabolic reprogramming drives nutrient flux in diabetic complications. *JCI Insight* **1**, e86976.

Schmuth, M., Moosbrugger-Martinz, V., Blunder, S. and Dubrac, S. (2014) Role of PPAR, LXR, and PXR in epidermal homeostasis and inflammation. *Biochim. Biophys. Acta* **1841**, 463-473.

Shiba, E., Izawa, K., Kaitani, A., Isobe, M., Maehara, A., Uchida, K., Maeda, K., Nakano, N., Ogawa, H., Okumura, K., Kitamura, T., Shimizu, T. and Kitaura, J. (2017) Ceramide-CD300f binding inhibits lipopolysaccharide-induced skin inflammation. *J. Biol. Chem.* **292**, 2924-2932.

Simpson, E. L., Chalmers, J. R., Hanifin, J. M., Thomas, K. S., Cork, M. J., McLean, W. I., Brown, S. J., Chen, Z., Chen, Y. and Williams, H. C. (2014) Emollient enhancement of the skin barrier from birth offers effective atopic dermatitis prevention. *J. Allergy Clin. Immunol.* **134**, 818-823.

Smith, S., Witkowski, A. and Joshi, A. K. (2003) Structural and functional organization of the animal fatty acid synthase. *Prog. Lipid Res.* **42**, 289-317.

Tawada, C., Kanoh, H., Nakamura, M., Mizutani, Y., Fujisawa, T., Banno, Y. and Seishima, M. (2014) Interferon-gamma decreases ceramides with long-chain fatty acids: possible involvement in atopic dermatitis and psoriasis. *J. Invest. Dermatol.* **134**, 712-718.

Uchida, Y. (2014) Ceramide signaling in mammalian epidermis. *Biochim. Biophys. Acta* **1841**, 453-462.

van Smeden, J., Janssens, M., Kaye, E. C., Caspers, P. J., Lavrijsen, A. P., Vreeken, R. J. and Bouwstra, J. A. (2014) The importance of free fatty acid chain length for the skin barrier function in atopic eczema patients. *Exp. Dermatol.* **23**, 45-52.

Yosipovitch, G., Hodak, E., Vardi, P., Shraga, I., Karp, M., Sprecher, E. and David, M. (1998) The prevalence of cutaneous manifestations in IDDM patients and their association with diabetes risk factors and microvascular complications. *Diabetes Care* **21**, 506-509.